VII.B.6 Montana PEM Membrane Degradation Study*

Lee H. Spangler
Montana State University
207 Montana Hall
Bozeman, MT 59717
Phone: (406) 994-2891; Fax: (406) 994-2893; E-mail: spangler@montana.edu

Dan Stevenson
CTA
1500 Poly Drive, PO Box 1439
Billings, MT 59103
Phone: (406) 248-7455; E-mail: dans@ctagroup.com

DOE Technology Development Manager: Amy Manheim
Phone: (202) 586-1507; Fax: (202) 586-9811; E-mail: Amy.Manheim@ee.doe.gov

DOE Project Officer: Carolyn Elam
Phone: (303) 275-4953; Fax: (303) 275-4788; E-mail: Carolyn.Elam@go.doe.gov

Contract Number: DE-FG36-99GO10436

Start Date: April 16, 1999
Projected End Date: September 30, 2006

*Congressionally directed project

Objectives

- Develop a system capable of measuring current and voltage performance for each membrane in a proton exchange membrane (PEM) fuel cell stack and record the performance of each cell.
- Develop a single-cell PEM fuel cell to allow *in situ* synchrotron x-ray measurements of the cell in operation and to perform spatially resolved x-ray measurements on fuel cell elements before and after degradation.
- Perform magnetic resonance microimaging experiments on membrane materials.

Technical Barriers

This project addresses the following technical barriers from the Fuel Cells section of the Hydrogen, Fuel Cells and Infrastructure Technologies Program Multi-Year Research, Development and Demonstration Plan:

- A. Durability
- J. Startup Time/Transient Operation

Technical Targets

This project is conducting fundamental studies of PEM membrane electrode assembly (MEA) degradation. Insights gained from these studies will be disseminated to assist MEA manufacturers in understanding degradation mechanisms and working towards DOE 2010 fuel cell durability targets:

- Durability: 5,000 hrs
- Number of starts: 20,000

Approach

- Design a system to capture individual cell performance in real time (current, voltage, temperature points taken every 0.5 millisecond).
- Test the stack response as it is subjected to load transients. Monitor each cell in the stack for its entire lifetime.
- As failures occur, analyze the cell using x-ray techniques, including methods that provide spatial resolution and chemical composition information.
- As failures occur, analyze the membrane material using magnetic resonance imaging (MRI) to get membrane permeability information.
- Search electrical records of failed membranes to see if mode of failure or an electrical signature of failure can be discerned.

Accomplishments

- Fully instrumented 2 separate 80-membrane PEM fuel cells to acquire voltage-current (V-I) data at 2 kHz.
- Generated significant performance degradation in several MEAs over a four-month span.
- Concluded study reproducing bulk nuclear magnetic resonance (NMR) study of Nafion® 117 solvent mobility dependence on methanol (MeOH) concentration.
- Used MRI to unearth a large spatial heterogeneity in membrane material.
- Using spatially resolved x-ray analysis of membranes before and after degradation, showed no change in chemical makeup but a spatially non-uniform increase in membrane densification.

Future Directions

- Continue to operate instrumented fuel cells under increasingly severe load transients and determine performance degradation of cells.
- Process electrical response data and look for a "signature" of future degradation.
- Construct an electrophoretic NMR probe.
- Perform combined sequential MRI and x-ray analysis of membranes.

Introduction

The Montana State University (MSU) PEM membrane degradation project is geared towards determining how and why membranes in fuel cells degrade and fail. By monitoring every individual membrane in a fuel cell 2000 times/sec while the cell is subjected to real-world type use, we hope to 1) cause the types of degradation users see, but in a controlled environment; 2) determine an electrical signature that will identify what causes failure, or at least warn of impending failure; 3) perform advanced x-ray and MRI characterization of the degraded membranes to provide information that may result in improvements of the membrane material; and 4) perhaps allow design of electronic control systems that will prevent fuel cells from operating under conditions where damage is likely to occur. Our project has three interdependent components: 1) NMR microscopy of polymer electrolyte membranes; 2) synchrotron-based x-ray characterization of membranes; and 3) fuel cell electrical characteristics monitoring.
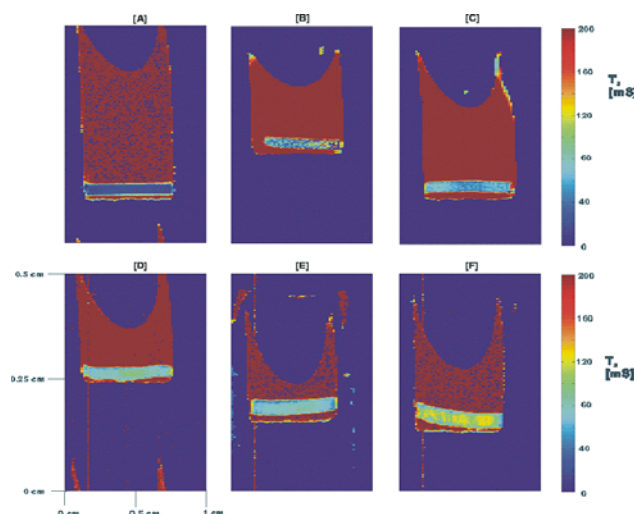
Results

NMR Microscopy of Polymer Electrolyte Membranes

Images of solvent magnetic relaxation and diffusion in Dupont Nafion® 117 PEMs have been used to characterize the molecular heterogeneity of the PEM over macroscopic (1 mm) scales. While bulk NMR measurements of electroosmotic mobility

[1], magnetic relaxation [2] and molecular self-diffusion of water [3] within PEMs have been reported, to our knowledge, the images generated by this project are the first spatially resolved images of solvent within a PEM.

T_2 Measurements Measuring the T_2 relaxation time of a sample gives quantitative data about how much solvent the polymer has absorbed. Better solvent absorption leads to more liquid within the sample, which in turn leads to longer T_2 times measured within the polymer. However, these longer T_2 times are not purely due to solvent uptake. As the membrane swells, it allows for more solvent to be adsorbed into the polymer. But, at the same time, the size of the flow channels increases. This allows the overall mobility of the solvent within each sample to increase. T_2 times also increase as the density of the polymer decreases due to swelling. Figure 1 shows the first spatially resolved measurements of the T_2 magnetic relaxation for fully saturated Nafion[®] submerged in solvent. The data clearly show the

increased swelling and solvent mobility as the mole fraction of MeOH is increased.

Diffusion Measurements To visualize the swelling and spatial distribution of molecular translational motion, diffusion as a function of methanol concentration is spatially resolved in diffusion maps. Using the same scaling factors, and placing diffusion maps side by side, Figure 2 shows a representative sample at each concentration.

The diffusion coefficient for samples in pure water starts out at a relatively high value. It decreases to a minimum in the 0.2 to 0.4 mol fraction methanol range, then increases. The decrease and linear increase are approximately equal in scale to those seen in Hietala *et al.* [3], in which bulk NMR measured diffusion over much larger membrane samples than used in this work. The variations between the Hietala *et al.* [3] data and this work are due to the heterogeneity of the PEMs. The spatially resolved data include spatial variations in the PEM, while in the larger PEM samples of Hietala *et al.* [3], the spatial heterogeneity is averaged out.

Material Inhomogeneity If a perfectly homogenous sample of Nafion[®] 117 were prepared as a single unit, the T_2 values across the membrane
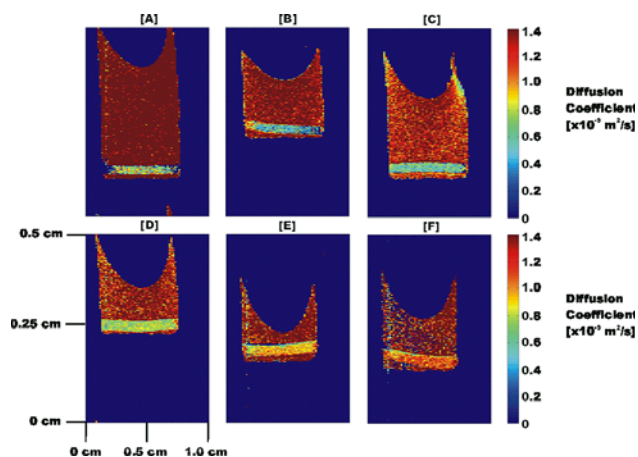

Figure 1. T_2 maps for the various methanol concentrations. A, B, C, D, E, and F correspond to 0, 0.2, 0.4, 0.6, 0.8, and 1.0 mol fraction methanol, respectively. As the concentration increases, the amount of free solution within the polymer also increases, as can be seen by the transition from dark blue in the pure water sample to yellow in the pure methanol sample. Membrane swelling can also be observed to increase with increasing methanol. Material inhomogeneity can be most clearly seen in samples B and C.

Figure 2. Diffusion maps for the various methanol concentrations. A, B, C, D, E, and F correspond to 0, 0.2, 0.4, 0.6, 0.8, and 1.0 mol fraction methanol, respectively. As can be seen, the diffusivity starts out as slightly higher within the polymer, dips slightly at 0.2 mol fraction, and then increases steadily as the methanol concentration increases.
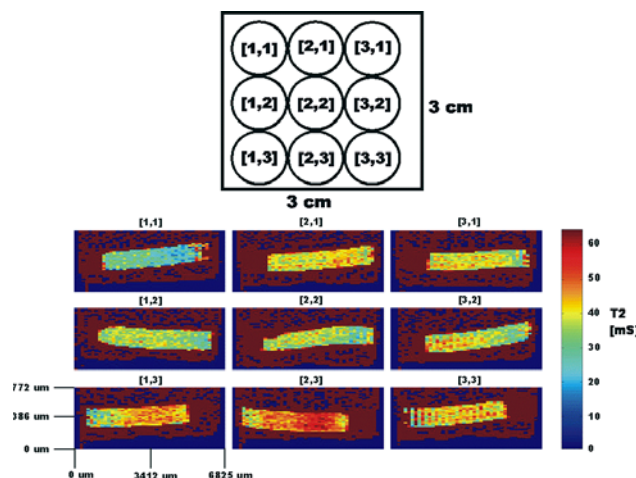
would be equal and constant everywhere. Any sample taken from this unit would show the exact same T_2 values, and there would be no deviation at any point. A T_2 map would show a single band of color, and the color would be exactly the same no matter where the sample was taken. This is not the case observed. At the beginning of the PEM study, the prepared Nafion[®] samples demonstrated extremely variable molecular mobility from sample to sample. All systematic errors in the preparation procedure were identified and eliminated, but the variations persisted. Some samples would show short T_2 relaxation times within the membrane, while other samples prepared in exactly the same manner would show long T_2 times.

In order to test the material homogeneity of Nafion[®] 117, a single 3 cm by 3 cm square was prepared according to the sample preparation of Hietala et al.[3]. The membrane was soaked in 0.2 mol fraction methanol for 24 hours. The sample sheet was notched at the top and on the right side in order to maintain the proper face-up orientation of all samples. Individual samples were punched from the membrane according to the diagram shown in Figure 3.

The resulting maps were cropped to show only the membrane and the immediate surroundings. The results of the longitudinal mapping are shown in Figure 3, and the transverse mapping data was also acquired (not shown). The level of molecular mobility variation is approximately equal in both directions, and the T_2 values within the membranes range from 20 ms in [1,1] to 60 ms in [2,3]. Since the samples are only 5 mm in diameter, this means that there is a molecular mobility difference equal to a factor of three in samples only 10 mm apart. In sample [1,3], the T_2 values range from 20 ms to 60 ms within the individual sample itself. This shows that the material inhomogeneity as measured by solvent molecular mobility is not confined to the millimeter length scale, but can vary significantly on a 20 micron length scale, which is the spatial resolution of these experiments.
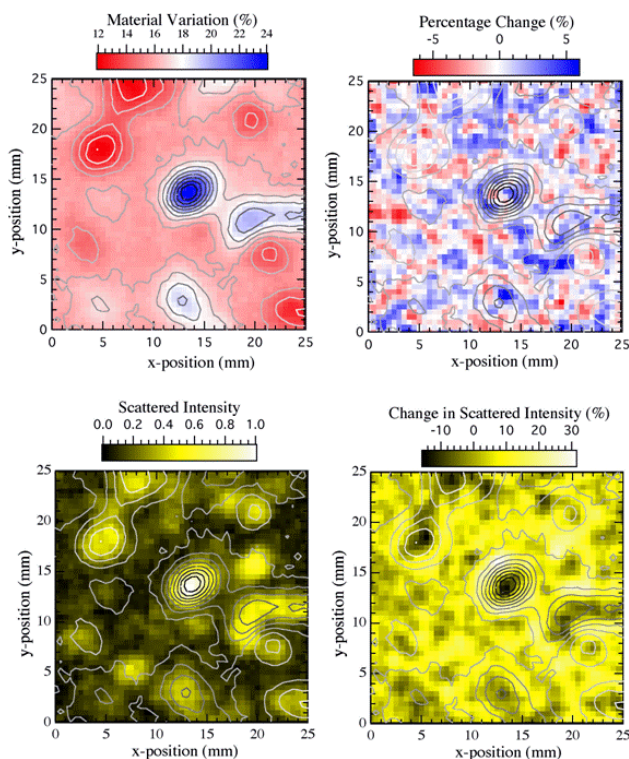
Synchrotron-Based X-Ray Characterization of Membranes

Scanning x-ray absorption, transmission, and small angle scattering data have been recorded on

Figure 3. Punch scheme and T_2 maps in the longitudinal direction for the material inhomogeneity experiment show that solvent T_2 values can vary significantly on both millimeter and 10 micron length scales. Number designations correspond to standard matrix notation. Longitudinal direction is from top to bottom, while transverse direction is from left to right. All samples were notched at the top (0°) and double notched at the right side (90°) to maintain orientation.

PEM membranes with 0.5 mm spatial resolution to determine chemical variation, thickness variation, and polymer density variation, respectively. Measurements were made at the MSU x-ray nanomaterials characterization facility at beamline U4B and beamline X23 of the National Synchrotron Light Source. A PEM was measured before and after a 3-month operational period which included repeated hydration and drying of the membrane. After use, the membrane showed nearly identical chemical make-up, except for a small spatially uniform sulfur component (10% variation across the membrane). Figure 4 shows four panels which address the PEM material and density variation after use. The upper left panel (red-to-blue color scheme) is a measure of the hard x-ray transmission through an unused membrane, which is a direct measure of the total material variation (thickness multiplied by density). The measurement shows that the total material can vary by almost a factor of two across a one-square-inch membrane. The bottom left panel (yellow color scheme) displays the spatially resolved intensity of x-rays scattered at a small angle from the straight through beam and is an indirect measure of

Figure 4. X-ray images showing PEM material and density variation after use. The upper left panel (red-to-blue color scheme) is a measure of the hard x-ray transmission through an unused membrane, which is a direct measure of the total material variation (thickness multiplied by density). The measurement shows that the total material can vary by almost a factor of two across a one-square-inch membrane. The bottom left panel (yellow color scheme) displays the spatially resolved intensity of x-rays scattered at a small angle from the straight through beam and is an indirect measure of the structure variation of the membrane (including density). Overlayed on all panels is a contour plot of the material variation (left top panel) to aid in making comparisons between panels.

the structure variation of the membrane (including density). Overlayed on all panels is a contour plot of the material variation (left top panel) to aid in making comparisons between panels. The correlation between the material variation and the scattered intensity suggests that the material variation is due mostly to changes in density and not due to changes in thickness of the membrane, suggesting that the density (and/or porosity) may be varying by

almost a factor of two. This is consistent with the NMR measurements showing dramatic variations in hydronium mobility (which, among other things, depends on density). This membrane was placed into our single-cell PEM fuel cell, and after a marked degradation of the fuel cell performance (50% power delivery reduction), the spatially resolved hard x-ray transmission was again measured. The material variation shows no major changes (±5% change), but there is a dramatic change in the x-ray scattered intensity (up to 30% increase). This change in scattered intensity is indicative of a densification of the membrane with use.
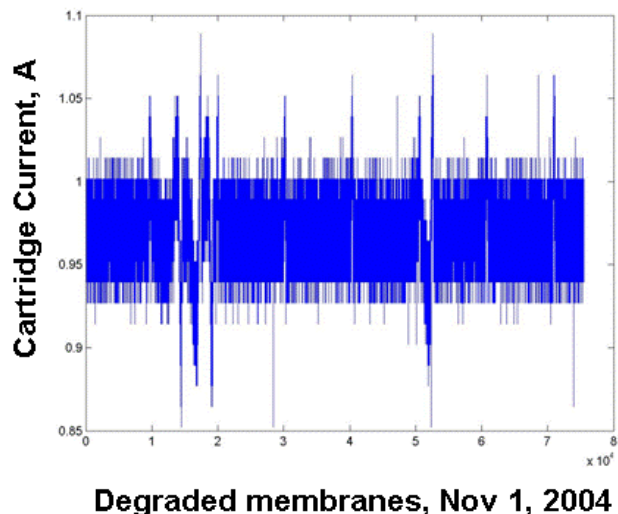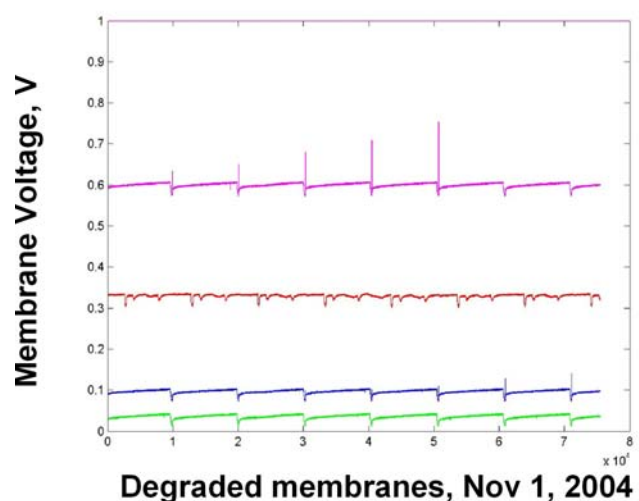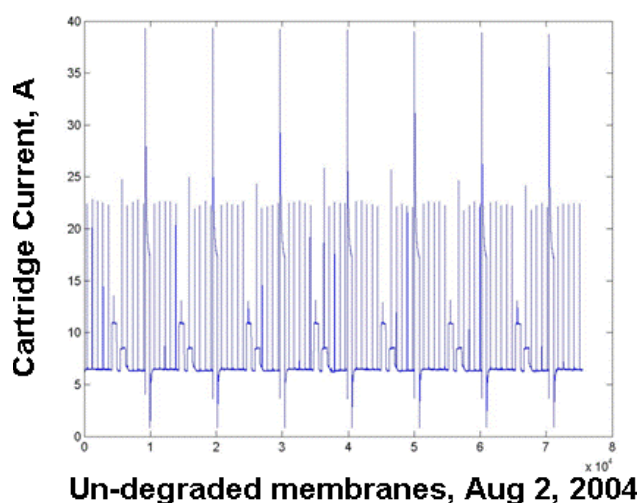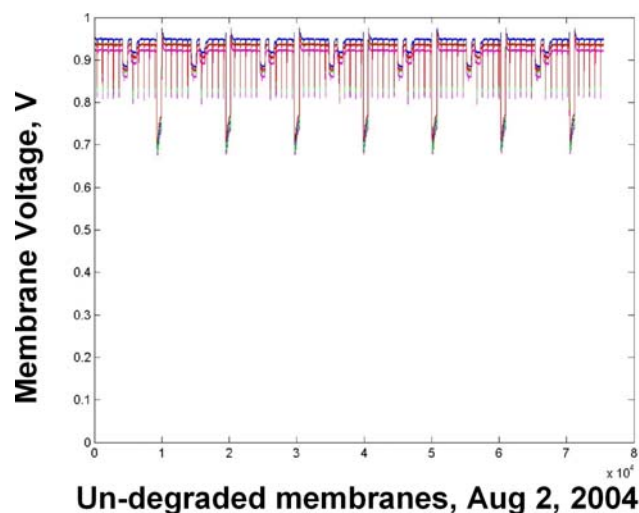
Fuel Cell Electrical Characteristics Monitoring

The fuel cell enclosures have been fully instrumented with in-house-designed A-D converters that monitor current and voltage for each individual cell at a 2000 Hz sampling rate. By simultaneously monitoring 80 to 160 cells (one or two enclosures), we hope to identify dominant failure modes. Because this generates over 5 billion data points per cell per month, we are in the very early stages of data analysis. We present some of the data and early analysis below.

Cartridge #1833 starts out with all membranes in roughly equivalent condition on August 2, 2004. Then, the performance of one membrane degrades precipitously, as indicated by the voltage collapse during periodic shorting (Figure 5). Figure 6 shows the initial current conditions. On September 20, 2004, the membranes are once again roughly equivalent in voltage, but the current waveform for that date indicates that this cartridge is carrying essentially no current. The cartridges are connected in parallel. The only effect that perturbs the cartridge voltage is the periodic shorting. We are suspicious that we have a DC offset on the last current plot for this cartridge because the current change is so small, but it is interesting that the membrane with the highest voltage is the one that initially seemed to be showing premature degradation.

In a second cartridge (#1865, data not shown), one membrane shows significantly worse performance in the newly installed condition. This membrane appears to improve slightly in the second voltage snapshot, but a quick check of the current

Figure 5. Four Membranes from Cartridge 1 (Serial #
1833) Under Observation Showing Voltage
Changes Over Time

Figure 6. Current Performance of the Same Four
Membranes Showing Degraded Performance
Over Time

indicates that the peak currents during shorting
decreased. In effect, the degradation of the other
membranes is forcing less current through the most
degraded one, so the voltage does not fall so much
when shorting. The third voltage graph shows one
membrane significantly worse off, and on the fourth
plot this cartridge shows no response. This is also an
interesting failure mode, and it is unclear how it
happened. Notice that the current actually increases
for this cartridge during the periodic shorting on the
final plot, but there is no component of the excitation
current. This suggests that other cells (in parallel)
are handling the load.

We are observing two phenomena. First, the
individual membranes are clearly failing in the
presence of a challenging load. We hope to use the
extensive membrane-by-membrane data to
understand how this works. Second, there is a very
significant interaction between membranes in series
and parallel connections. Depending on the
condition of a membrane's neighbors, load-
dependent degradation may change simply because
the distribution of the load is different.

Conclusions

The three-pronged approach shows promise for
yielding insights to degradation mechanisms and the
changes in materials properties that result.

- First-time spatially resolved MRI data of solvent mobility in saturated Nafion® 117 PEMs has been generated, reproducing bulk NMR measurements.

- MRI measurements of Nafion® 117 PEMs indicate significant spatial heterogeneity in the molecular mobility of solvent within the PEM on mm to μm scales, a result not attainable to our knowledge by any other technique.

- Via x-ray, a small, spatially homogeneous sulfur concentration was found on the membrane after it had degraded. The major change was a spatially inhomogeneous densification of the PEM. This densification was co-localized with the original density variations in the PEM.

- Individual membranes are clearly failing in the presence of a challenging load. We hope to use the extensive membrane-by-membrane V-I data to understand how this works.

- There is a very significant interaction between membranes in series and parallel connections. Depending on the condition of a membrane's neighbors, load-dependent degradation may change simply because the distribution of the load is different.

FY 2005 Publications/Presentations

1. Lussier, D. Larsen, and Y.U. Idzerda; "Performance of an X-ray Compatible Cell for Fuel Cell Material Characterization" (2004 – submitted).

2. Chen, D. Resnick, E. Negusse, and Y.U. Idzerda; "Identification of Mechanisms for PEM Membranes by Power Utilization Curve Analysis," Hydrogen, Fuel Cells & Infrastructure Technologies Review, Bozeman, MT (2004).

3. Invited Lecture: J.D. Seymour; "Magnetic Resonance Microscopy of Scale Dependent Transport Phenomena in Bioreactors and Polymer Electrolyte Membranes," 1st International Symposium on Micro & Nano-Scale Sensing Techniques for Energy and Bio System, Keio University, Yokohama, Japan, September 14, 2004.

4. D.T. Howe, J.D. Seymour, S.L. Codd, S.C. Busse and E.S. Peterson; "NMR Microscopy of Material Inhomogeneity in Polymer Electrolyte Membranes (PEMs)," accepted poster 8th International Conference on Magnetic Resonance Microscopy, Utsunomiya, Japan, August 22-25, 2005.

5. S.R. Shaw; "Instrumentation for PEM Fuel Cell Transient Degradation Monitoring," Proceeding of the IEEE PES General Meeting, Denver, CO (2004).

References

1. M. Ise, K.D. Kreuer, and J. Maier, Electroosmotic drag in polymer electrolyte membranes: an electrophoretic NMR study. Solid State Ionics, 125: 213-223 (1999).

2. B. MacMillan, A.R. Sharp, and R.L. Armstrong, An NMR investigation of the dynamical characteristics of water absorbed in Nafion. Polymer, 40: 2471-2480 (1999).

3. S. Hietala, S.L. Maunu, and F. Sundholm, Sorption and diffusion of methanol and water in PVDF-g-PSSA and Nafion 117 polymer electrolyte membranes. Journal of Polymer Science, Part B: Polymer Physics, 38: 3277-3284 (2000).